Structural Health Monitoring
http://shm.sagepub.com/

Multiple crack damage detection of structures using the two crack transfer matrix

P Nandakumar and K Shankar

Structural Health Monitoring published online 20 May 2014
DOI: 10.1177/1475921714532993

The online version of this article can be found at:
http://shm.sagepub.com/content/early/2014/05/14/1475921714532993

Published by:
SAGE
http://www.sagepublications.com

Additional services and information for *Structural Health Monitoring* can be found at:

Email Alerts: http://shm.sagepub.com/cgi/alerts

Subscriptions: http://shm.sagepub.com/subscriptions

Reprints: http://www.sagepub.com/journalsReprints.nav

Permissions: http://www.sagepub.com/journalsPermissions.nav

Citations: http://shm.sagepub.com/content/early/2014/05/14/1475921714532993.refs.html

>> OnlineFirst Version of Record - May 20, 2014

What is This?

Downloaded from shm.sagepub.com at UNIVERSITE LAVAL on July 13, 2014

Original Article

SHM Structural Health Monitoring

Structural Health Monitoring
1–14
© The Author(s) 2014
Reprints and permissions:
sagepub.co.uk/journalsPermissions.nav
DOI: 10.1177/1475921714532993
shm.sagepub.com
SAGE

Multiple crack damage detection of structures using the two crack transfer matrix

P Nandakumar and K Shankar

Abstract

A damage detection scheme for multiple crack detection in beams is presented, based on a transfer matrix derived from beam element with two cracks. Based on fracture mechanics principles, a crack is modelled as a hinge, which provides an additional flexibility to the element. Each element is assumed to have two open-edge cracks and a new transfer matrix called two crack transfer matrix is developed using finite element method. Using an inverse approach, the transfer matrix is used to predict cracks in a beam. The state vector at a node includes displacements, forces and moments at that node; when it is multiplied with the transfer matrix, the state vector at the adjacent node can be obtained. The state vector formed at the starting node, known as initial state vector, needs to be estimated, from which state vectors at adjacent nodes are predicted using the transfer matrix. Displacement responses are measured at a few adjacent nodes in the structure. The mean square error between measured and predicted responses is minimized using a heuristic optimization algorithm, with crack depth and location in each element as the optimization variables. Two numerical examples, a cantilever and a sub-structure of a frame with nine members, are solved with two cracks in each element. The damage detection method is also validated experimentally by local identification of sub-structure of a fixed beam where the initial state vector is measured using strain gauges and accelerometers. Using this method, two cracks per single element were successfully identified. The two crack transfer matrix method is suitable for local damage identification in large structures.

Keywords

Two crack transfer matrix, state vector, damage detection, successive identification, particle swarm optimization

Introduction

Structural health monitoring (SHM) is a process by which the health of the structure is predicted using non-destructive approach. It is highly essential for civil, mechanical and aerospace structures, which undergo repeated cyclic loading after an impact loading or earthquake. Even small breathing cracks in the structural element may cause an unexpected loss; hence, it must undergo SHM process periodically. Generally, the crack detection process such as ultrasonic methods, optical methods, radiography, magnetic field methods, eddy-current methods and thermal field methods is used for damage detection. These methods are expensive and require that the zone of the damage is known a priori, and that the structural element to be inspected is accessible. As an alternate, vibration-based damage detection methods deserve further investigation.

Damage in the machine element or structure means not only the presence of discontinuities in the material but also include changes in the boundary conditions, loose machine fittings or fasteners such as bolts and nuts. The damage provides a local flexibility in the structural element, which reduces the natural frequency of the entire structure and dynamic responses as well. Gounaris and Dimarogonas[1] developed elemental compliance matrix for cracked beam element by assuming the crack increases the flexibility of the element due to strain energy concentrations in the vicinity of the crack tip under load. From that compliance matrix, elemental stiffness and mass matrices have been developed, and using them, the forced vibrational behaviour of a

Department of Mechanical Engineering, Indian Institute of Technology Madras, Chennai, India

Corresponding author:
K Shankar, Department of Mechanical Engineering, Indian Institute of Technology Madras, Chennai 600036, India.
Email: skris@iitm.ac.in

Downloaded from shm.sagepub.com at UNIVERSITE LAVAL on July 13, 2014

cantilever with open crack was studied. Chondros et al.[2] developed a continuous cracked beam theory for Euler–Bernoulli beams with single- and double-open-edge cracks. The crack was modelled as a continuous flexibility using the displacement field in the vicinity of the crack. Zheng and Kessissoglou[3] developed an overall stiffness matrix from the overall additional flexibility matrix rather than local additional flexibility matrix by which a better natural frequency and mode shape of structures were found. Krawczuk et al.[4] developed new finite element (FE) matrices for cracked beam elements using elasto-plastic fracture mechanics. FE procedure was applied with suitable boundary conditions at the crack with two different polynomial functions. Viola et al.[5] developed a new prismatic Timoshenko beam element with crack, and the effect of crack in stiffness and mass matrices was investigated. Khiem and Lien[6] determined natural frequencies of cantilever with multiple cracks using transfer matrix (TM) approach. Gounaris et al.[7] formulated compliance matrix for Timoshenko-cracked beam element by which identified crack in a cantilever by measuring coupled response. However, it is suitable for only one edge crack present in the beam, and it requires lot of nomograms for each frequency of vibration. Krawczuk[8] detected the crack in beam-like structures using wave propagation method using genetic algorithm (GA) and gradient search technique. Gao and Lu[9] used residual generation approach in measured acceleration response for damage detection in structural members.

Tee et al.[10] identified crack on 50 degree-of-freedom (DOF) shear model using observer Kalman filtre identification (OKID) and eigen realization algorithm (ERA)-based condensed model identification and recovery (CMIR) technique with global and substructural (SS) approach using GA. It has been proved that the SS approach identifies crack with better accuracy than the global structure approach. Prashanth and Shankar[11] detected damage on structures using a two-stage artificial neural network technique. Damages on a 6-story shear building, a 9-member frame structure and a 30-member frame were identified. Varghese and Shankar[12] identified cracks in a SS of the cantilever using combined acceleration matching and transient power flow balance. Philips et al.[13] identified damage in beams using displacement modes and distributed strain measurement. In the above algorithms, for each iteration, the large system matrices need to be solved, which consumes more computational time. As an alternative, TM and state vectors are introduced in this article. The size of the TM does not increase with respect to the total number of DOF of the model, thus reducing the computational effort.

Liew et al.[14] used TM in the field of rotor dynamics for transient response analysis of non-symmetrical unbalance flexible rotor. Ghasemalizadeh et al.[15] determined natural frequency and frequency responses for multirotor system supported on two bearings using TM. To the best of the author's knowledge, Nandakumar and Shankar[16] were the first to propose using TM as an inverse problem for local identification in structures. They used TMs based on lumped mass and also consistent mass approaches to identify parameters of beam structures. Later, Nandakumar and Shankar[17,18] extended the work to damped TMs and experimentally verified the TM-based identification strategy. The novelties of the present work are the following: (1) the above TM method is extended to crack identification and (2) a formulation is derived to identify two cracks per beam element, which is hitherto not reported in the literature.

Beam element with two cracks

A beam element of length l_e is considered with two cracks located at a distance of l_1 and l_2 from its left-end node, as shown in Figure 1.

Let a_1 and a_2 be the depth of the cracks measured from the top of the element. The cross-sectional dimension of the beam section is $b \times h$. The non-dimensional crack parameters normalized crack depth (ξ) and location (λ) are defined as $\xi_1 = a_1/h$, $\xi_2 = a_2/h$, $\lambda_1 = l_1/l_e$ and $\lambda_2 = l_2/l_e$. P_1 and P_2 are the transverse force and moment, respectively, applied at the right node on the cracked element. The flexibility due to the crack in the beam element can be obtained by Castigliano's theorem

$$c_{ij} = \frac{\partial^2 U}{\partial P_i \partial P_j} \tag{1}$$

for $i = 1, 2$ and $j = 1, 2$, where U be the strain energy in the cracked beam element and P_i be the nodal forces applied on the element. Strain energy U in the cracked beam element is given by the relation

$$U = \int_A J dA \tag{2}$$

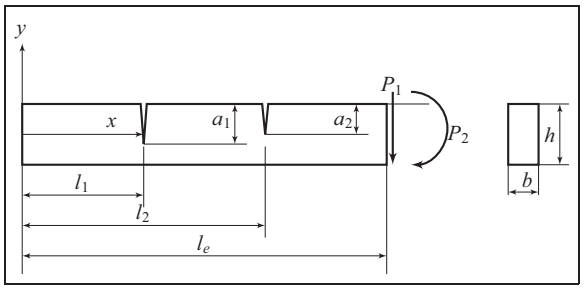

Figure 1. Beam element with two cracks.

Downloaded from shm.sagepub.com at UNIVERSITE LAVAL on July 13, 2014

where A is the crack area and J is the strain energy density function, which is given by the relation[4]

$$J = \frac{1}{E'}\left[\left(\sum_{k=1}^{6} K_{I,k}\right)^2 + \left(\sum_{k=1}^{6} K_{II,k}\right)^2 + \left(\sum_{k=1}^{6} K_{III,k}\right)^2\right] \tag{3}$$

where $E' = E/(1-\nu^2)$ and K_I, K_{II} and K_{III} are stress intensity factor corresponding to the first, second and third mode of the crack formation, respectively, where ν is Poisson's ratio and E is Young's modulus of the beam material. k is DOF at the node. Since the crack element considered is the pure bending beam element, the effect of first mode of the crack is predominant and the second and third modes are neglected. Equation (3) can be deduced as

$$J = \frac{1-\nu^2}{E}\left(\sum_{k=1}^{2} K_{I,k}\right)^2 \tag{4}$$

Substituting the above equation in equation (1)

$$c_{ij} = \frac{1-\nu^2}{E}\frac{\partial^2}{\partial P_j \partial P_i}\int_A \left(\sum_{k=1}^{2} K_{I,k}\right)^2 dA \tag{5}$$

The cross-section of the cracked beam element is shown in Figure 2. Let α be the crack depth that varies from 0 to a at the cracked section. The stress intensity factor at any crack depth α is given by $K_I = \sigma\sqrt{\pi\alpha} f(\alpha/h)$, where σ be the bending stress at the cracked section which is $\sigma = My/I$, where M is the bending moment, y is the distance of the layer from its neutral axis and I is area moment of inertia. For a rectangular cross-section, the bending stress at the extreme layer of the section may be calculated as

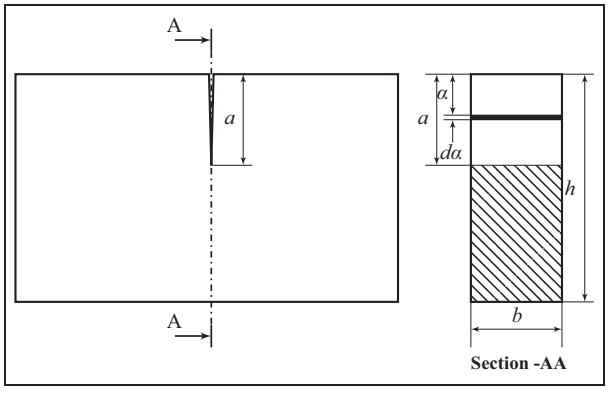

Figure 2. Cross-section at the crack.

$\sigma = 6M/(bh^2)$, and $f(\alpha/h)$ is the geometric correction function, which is given by[4]

$$f(\alpha/h) = \sqrt{\frac{tan(\pi\alpha/2h)}{\pi\alpha/2h}}\frac{0.923 + 0.199[1 - sin(\pi\alpha/2h)]^4}{cos(\pi\alpha/2h)} \tag{6}$$

Consider a rectangular strip of thickness $d\alpha$ at a distance α from the top of the cracked section as shown in Figure 2. The area of the strip is $dA = bd\alpha$. Let normalized crack depth $\bar{\alpha} = \alpha/h$, substituting in equation (5)

$$c_{ij} = \frac{36\pi(1-\nu^2)}{Ebh^2}\frac{\partial^2(P_1(1-l_1)+P_2)^2}{\partial P_j \partial P_i}\int_0^{\xi} \bar{\alpha} f(\bar{\alpha})^2 d\bar{\alpha} \tag{7}$$

from equation (7)

$$\begin{aligned} c_{11} &= \tfrac{6\pi h(1-\nu^2)((1-\lambda)l_e)^2}{EI}\int_0^{\xi} \bar{\alpha} f(\bar{\alpha})^2 d\bar{\alpha} \\ c_{12} = c_{21} &= \tfrac{6\pi h(1-\nu^2)(1-\lambda)l_e}{EI}\int_0^{\xi} \bar{\alpha} f(\bar{\alpha})^2 d\bar{\alpha} \\ c_{22} &= \tfrac{6\pi h(1-\nu^2)}{EI}\int_0^{\xi} \bar{\alpha} f(\bar{\alpha})^2 d\bar{\alpha} \end{aligned} \tag{8}$$

If the element is applied with only force, P_1, c_{12} and c_{22} vanish, and hence, $c = c_{11}$.

FE formulation

The additional flexibilities of the open cracks can be obtained from equation (9), the stiffness and mass matrices of the beam element with two cracks can be obtained by FE procedure. The cracked beam element, which is shown in Figure 1, is considered as three segments connected by two massless hinges of flexibility c_1 and c_2, respectively, as shown in Figure 3.

Let $w(x)$ and $\theta(x)$ be the transverse displacement and angular displacement, respectively, about an axis perpendicular to the plane containing the element, respectively. Three different polynomials are assumed for the field variables of this element since it has three different segments

$$\begin{aligned} &w_1(x) = a_1 + a_2 x + a_3 x^2 + a_4 x^3; \\ &\theta_1(x) = w'_1(x) = a_2 + 2a_3 x + 3a_4 x^2; \quad 0 \leqslant x \leqslant l_1 \\ &w_2(x) = a_5 + a_6 x + a_7 x^2 + a_8 x^3; \\ &\theta_2(x) = w'_2(x) = a_6 + 2a_7 x + 3a_8 x^2; \quad l_1 \leqslant x \leqslant l_2 \\ &w_3(x) = a_9 + a_{10} x + a_{11} x^2 + a_{12} x^3; \\ &\theta_3(x) = w'_3(x) = a_{10} + 2a_{11} x + 3a_{12} x^2; \; l_2 \leqslant x \leqslant l_e \end{aligned} \tag{9}$$

Downloaded from shm.sagepub.com at UNIVERSITE LAVAL on July 13, 2014

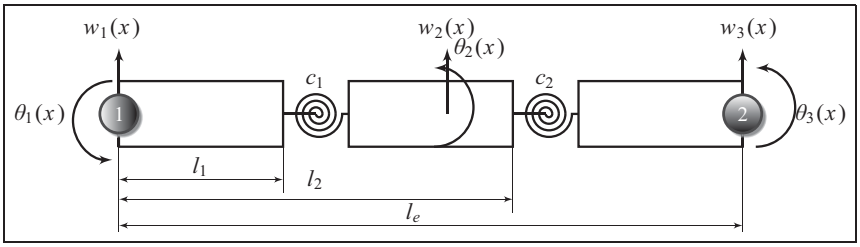

Figure 3. Equivalent model of cracked beam element.

where a_1–a_{12} are the constants. The following are the nodal values and conditions applied to the cracked beam element

$$
\begin{aligned}
&w_1(0) = W_1;\ \ \theta_1(0) = \phi_1;\ \ w_3(l_e) = W_2;\ \ \theta_3(l_e) = \phi_2\\
&w_1(l_1) = w_2(l_1);\ \ w_1''(l_1) = w''_2(l_1);\ \ w_1'''(l_1) = w_2'''(l_1)\\
&w_2(l_2) = w_3(l_2);\ \ w_2''(l_2) = w_3''(l_2);\ \ w_2'''(l_2) = w_3'''(l_2)\\
&EIw''_2(l_1) = \frac{1}{c_1}(\theta_2(l_1) - \theta_1(l_1));\\
&EIw''_3(l_2) = \frac{1}{c_2}(\theta_3(l_2) - \theta_2(l_2))
\end{aligned}
\tag{10}
$$

where W_1, W_2, ϕ_1 and ϕ_2 are the displacement and slope at the nodes 1 and 2, respectively. The shape function matrix $[N(x)]$ of size 6×4 relates the nodal DOF with the field variables as follows

$$
\begin{Bmatrix} w_1(x)\\ \theta_1(x)\\ w_2(x)\\ \theta_2(x)\\ w_3(x)\\ \theta_3(x) \end{Bmatrix} = \begin{bmatrix} N_{11}(x) & N_{12}(x) & N_{13}(x) & N_{14}(x)\\ N_{21}(x) & N_{22}(x) & N_{23}(x) & N_{24}(x)\\ N_{31}(x) & N_{32}(x) & N_{33}(x) & N_{34}(x)\\ N_{41}(x) & N_{42}(x) & N_{43}(x) & N_{44}(x)\\ N_{51}(x) & N_{52}(x) & N_{53}(x) & N_{54}(x)\\ N_{61}(x) & N_{62}(x) & N_{63}(x) & N_{64}(x) \end{bmatrix} \begin{Bmatrix} W_1\\ \phi_1\\ W_2\\ \phi_2 \end{Bmatrix} \tag{11}
$$

in the above equation, the shape function matrix is written as $[N_1(x), N_2(x), N_3(x), N_4(x)]^T$ for simplicity. The suffixes 1–4 represent the respective row vector of the shape function matrix. The stiffness matrix and mass matrix for the two crack beam element are obtained as follows

$$
[K^e] = EI\left(\int_0^{l_1} B_1^T B_1 dx + \int_{l_1}^{l_2} B_2^T B_2 dx + \int_{l_2}^{l_e} B_3^T B_3 dx\right) \tag{12}
$$

$$
\begin{aligned}
&[M^e] = \rho A\\
&\left(\int_0^{l_1} N_1(x)^T N_1(x) dx + \int_{l_1}^{l_2} N_3(x)^T N_3(x) dx + \int_{l_2}^{l_e} N_5(x)^T N_5(x) dx\right)
\end{aligned}
\tag{13}
$$

where $B_1 = (d^2[N_1(x)])/dx^2$, $B_2 = (d^2[N_3(x)])/dx^2$ and $B_3 = (d^2[N_5(x)])/dx^2$. It can be seen that if $c_1 = c_2 = 0$, the matrices for uncracked beam element are obtained. The crack in the beam element has more influence in reduction of its stiffness, but it does not affect the mass distribution appreciably. Hence, the mass matrix for uncracked beam element can also be used.

TM formulation for two crack element

The characteristic equation for the second-order linear system is written for the two crack beam element shown in Figure 3

$$
[M^e]\{\ddot{q}(t)\} + [C^e]\{\dot{q}(t)\} + [K^e]\{q(t)\} = \{f(t)\} \tag{14}
$$

where $[M^e]$, $[K^e]$ and $[C^e]$ are elemental mass, stiffness and damping matrices of the two crack beam element, respectively, and $\{\ddot{q}(t)\}$, $\{\dot{q}(t)\}$, $\{q(t)\}$ and $\{f(t)\}$ are acceleration, velocity, displacement and excitation force vectors, respectively, at element nodes. Assume the material of the structure is lightly damped, the damping force is negligible when compared with other force. For a harmonic excitation force, the acceleration $\ddot{q}(t) = -\omega^2 q(t)$, where ω is circular frequency of excitation. Equation (14) becomes

$$
([K^e] - \omega^2[M^e])\{q(t)\} = \{f(t)\} \tag{15}
$$

Let $[D_c] = [K^e] - \omega^2[M^e]$ is the dynamic stiffness matrix for the cracked beam element. For equilibrium of the element shown in Figure 3, the above equation is written as

$$
\left\{\begin{array}{c} -M_1(t)\\ -V_1(t)\\ \hline M_2(t)\\ V_2(t) \end{array}\right\} = \left[\begin{array}{cc|cc} D_{c11} & D_{c12} & D_{c13} & D_{c14}\\ D_{c21} & D_{c22} & D_{c23} & D_{c24}\\ \hline D_{c31} & D_{c32} & D_{c33} & D_{c34}\\ D_{c41} & D_{c42} & D_{c43} & D_{c44} \end{array}\right] \left\{\begin{array}{c} w_1(t)\\ \theta_1(t)\\ \hline w_2(t)\\ \theta_2(t) \end{array}\right\} \tag{16}
$$

the state vector at node 1 $\{X_1\} = \{w_1(t), \theta_1(t), M_1(t), V_1(t)\}^T$ is a known vector, which can be obtained by rearranging force and response vectors of equation (16). Let

Downloaded from shm.sagepub.com at UNIVERSITE LAVAL on July 13, 2014

$$[D_1] = \begin{bmatrix} D_{c11} & D_{c12} \\ D_{c21} & D_{c22} \end{bmatrix}, \quad [D_2] = \begin{bmatrix} D_{c13} & D_{c14} \\ D_{c23} & D_{c24} \end{bmatrix},$$
$$[D_3] = \begin{bmatrix} D_{c31} & D_{c32} \\ D_{c41} & D_{c42} \end{bmatrix}, \quad [D_4] = \begin{bmatrix} D_{c33} & D_{c34} \\ D_{c43} & D_{c44} \end{bmatrix}$$
$$F(t) = \begin{Bmatrix} M(t) \\ V(t) \end{Bmatrix} \quad \text{and} \quad x(t) = \begin{Bmatrix} w(t) \\ \theta(t) \end{Bmatrix}$$

then equation (16) is written as

$$\begin{Bmatrix} -F_1(t) \\ F_2(t) \end{Bmatrix} = \begin{bmatrix} [D_1] & [D_2] \\ [D_3] & [D_4] \end{bmatrix} \begin{Bmatrix} x_1(t) \\ x_2(t) \end{Bmatrix} \tag{17}$$

from equation (17)

$$\begin{Bmatrix} x_2(t) \\ F_2(t) \end{Bmatrix} = \begin{bmatrix} -[D_2] & [0] \\ -[D_4] & [I] \end{bmatrix}^{-1} \begin{bmatrix} [D_1] & [I] \\ [D_3] & [0] \end{bmatrix} \begin{Bmatrix} x_1(t) \\ F_1(t) \end{Bmatrix} \tag{18}$$

where $[I]$ is an identity matrix and $[0]$ is a null matrix of size 2×2. The TM for two crack beam element (two crack transfer matrix (TCTM)) is given by

$$[T_c] = \begin{bmatrix} -[D_2] & [0] \\ -[D_4] & [I] \end{bmatrix}^{-1} \begin{bmatrix} [D_1] & [I] \\ [D_3] & [0] \end{bmatrix} \tag{19}$$

TM for multiple elements is calculated from elemental TMs. The state vector is estimated across n elements and state vector at node 1 $\{X_1\}$ is known, and then the internal response vector at the $(n+1)th$ node $\{X_{n+1,i}\}$ is given by

$$\{X_{n+1,i}\} = \left(\prod_{k=1}^{n} [T_{(n+1-k),(n+2-k)}] \right) \{X_{1,i}\} + \sum_{j=1}^{n} \left(\prod_{k=1}^{n+1-j} [T_{(n+1-k),(n+2-k)}] \right) \{X_{j,e}\} \tag{20}$$

where $\{X_{j,e}\}$ is external force vector at jth node.

Crack detection by TCTM method

Cracks in a structure are identified using the newly developed TCTM by assuming the mass and flexural rigidity of the beam are known and two open cracks are present in each element. The unknown parameters are the normalized crack depth (ξ) and the normalized crack location (λ). The structure is excited by a known harmonic force at a node. At a node on the structure where the identification is to begin, the state vector is estimated (i.e. initial state vector). This requires both accelerometers and strain gauges. Additionally, accelerations need to be measured at a few adjacent nodes. These are converted into displacements and compared with predicted values by TM.

After formation of the initial state vector, the state vectors are obtained at adjacent locations by pre-multiplying with elemental TCTM using equation (20). Since the crack parameters in the TMs are unknown, they are searched by particle swarm optimization (PSO) algorithm within the feasible range of 0–1. The zero value of identified normalized crack depth shows the undamaged state of an element. The successive identification strategy[16–18] is followed to identify crack parameters, where cracks are estimated progressively from starting node.

According to the successive identification strategy, the parameters of element(s) are identified between the nodes where the initial state vector is formed and its adjacent measured location. If a structure has n number of acceleration measurement locations and the initial state vector is formed at any location i, then the parameters of elements between ith and $(i+1)th$ measured locations are identified. The mean square error (MSE) between the predicted displacement responses for searched values of crack parameters and measured displacement responses at the ith location is minimized. The crack parameters for which the MSE between measured and predicted responses is minimum are the identified parameters of crack. The error function is given by

$$\varepsilon = \frac{\sum_{j=1}^{L} |w_m(j) - w_e(j)|^2}{L} \tag{21}$$

where $w_m(j)$ and $w_e(j)$ are measured and predicted displacement, respectively, at jth time step. L is the total number of time steps. This procedure is repeated until parameters of all the elements are identified. The parameters are identified successively from the initial location to end location using both complete and incomplete measurements. Complete measurement means that translational acceleration responses are measured at all nodes (angular acceleration is measured only at the node where the initial state vector is formed). However, the complete measurement is not possible for large structures in practice due to non-availability of large number of sensors. Hence, in practice, parameters are identified with a few sensors at selected nodes only, which is known as incomplete measurement. The accuracy is less than that of complete measurements, but the errors are within acceptable levels.[16–18]

Numerical examples

The damage detection method using TCTM is applied on two examples, which are based on numerically simulated experiments. A cantilever with four cracks and a SS of a nine-member structure, which contains four cracks, are identified by TCTM method. The structural

Downloaded from shm.sagepub.com at UNIVERSITE LAVAL on July 13, 2014

parameters such as mass and stiffness of the undamaged structure are assumed to be known, and the crack parameters normalized depth and location are identified. The structure is excited by known harmonic force at a point on the structure, and the acceleration responses are measured at few nodes and converted into displacement. All measured responses are numerically simulated using Newmark's constant acceleration method for a time length of 3 s. Gaussian white noise of 5% of the root mean square (RMS) value of the numerically simulated response is added with all measurements to simulate experimental errors.

Example 1: cantilever

A uniform slender cantilever of cross-section of 50 × 5 mm and length of 520 mm, which was used by Viola et al.,[19] is considered here with multiple cracks. Young's modulus of the beam material (E) is 206 GPa, and its density is 7850 kg/m^3. Four cracks of depths of 0.5, 1.5, 0.4 and 2.5 mm are located at 120, 150, 380 and 395.2 mm, respectively, from the fixed end of the cantilever, as shown in Figure 4. The normalized crack depths are $\xi_{c1} = 0.1$, $\xi_{c2} = 0.3$, $\xi_{c3} = 0.08$ and $\xi_{c4} = 0.5$, and their global locations are $\lambda_{c1} = 0.23$, $\lambda_{c2} = 0.288$, $\lambda_{c3} = 0.73$ and $\lambda_{c4} = 0.76$, respectively. The first natural frequency of the cracked beam is 15.07 Hz. The cantilever is divided into six elements. Cracks $C1$ and $C2$ are located in element 2, and $C3$ and $C4$ are located in element 5. The normalized crack locations in element 2 with respect to the left end of the element are $\lambda_{e21} = 0.384$ and $\lambda_{e22} = 0.73$, and the same in element 5 are $\lambda_{e51} = 0.384$ and $\lambda_{e52} = 0.56$. ($_{e21}$ represents crack 1 in element 2, that is, $C1$).

The free end of the cantilever is subjected to a harmonic excitation of $F(t) = 10\,sin(2\pi 10t)$ N. Acceleration responses are measured at all nodes, and angular acceleration response is measured only at free-end node. The initial state vector $\{X_7\} = \{w_7(t), \theta_7(t), 0, 0\}^T + \{0, 0, 0, F(t)\}^T$ is formed at node 7 since bending moment and shear force is 0 at that node. The crack parameters are searched between the values of 0 and 1 by PSO. State vector at node 6 is calculated by multiplying initial state vector with TCTM with predicted values of crack parameters of element 6. The MSE between measured and predicted responses is minimized by PSO with swarm size of 50 and number of iterations of 50 in each cycle of identification. In the next cycle, the crack parameters of element 5 is identified by considering the state vector $\{X_6\}$ as initial state vector and MSE is minimized at node 5. Thus, the identification cycle is repeated for all elements. The identified parameters with complete measurement are shown in Figure 5, and the percentage of absolute error in identified parameters of each crack is shown in Figure 6. The small breathing crack of depth 5% of beam height is identified with an absolute error of 0.87% with noise-free measurement and 5.87% with 5% noise level in measurements. The global location of the same crack is identified with an error of 0.016% without noise and 0.86% with 5% noise in measurements. The total time taken for the convergence is 14 s.

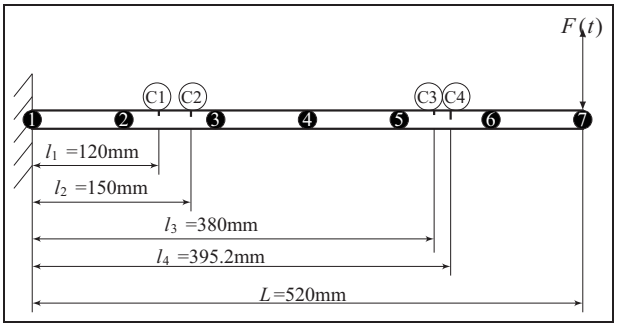

Figure 4. FE model of cantilever with multiple cracks.
FE: finite element.

The cracks are identified with responses measured only at nodes 2, 4, 6 and 7. The elements between the starting node and the adjacent measured node (node 6) are considered. The response is predicted at the adjacent node with predicted crack parameters using equation (20). The MSE between the measured and predicted responses is minimized by PSO with 50 swarm size and 100 iterations in each cycle (total 400 iterations). The identified parameters are shown in Figure 7, and the absolute percentage of error is shown in Figure 8. In this case, the crack depth of 5% of beam height is identified with an error of 4.44% with noise-free measurement and 9.87% at 5% noise level in measurements. The error in its location is 0.07% without noise and 0.65% with 5% noise. The time taken for incomplete measurement case is 19 s. The percentage of error is comparatively high at cracks with small magnitudes since they show very small amount change in the dynamic responses. Hence, it is concluded that TCTM method is identifying crack with good accuracy and speed.

Next, the results are compared with other published studies. Viola et al.[19] identified a single crack of depth of 50% of beam height, as located in this problem using a frequency-domain method from experimentally obtained measurements of unspecified noise content. The percentage of error in identification was 2.5% in crack depth and 0.53% in absolute crack location. The crack parameters identified by TCTM method for the same depth and location have an error of 0.21% in depth and 0.04% in absolute crack location using noise-free measurement. The errors are 0.87% in depth and 0.38% in location in the case of 5% noisy

Downloaded from shm.sagepub.com at UNIVERSITE LAVAL on July 13, 2014

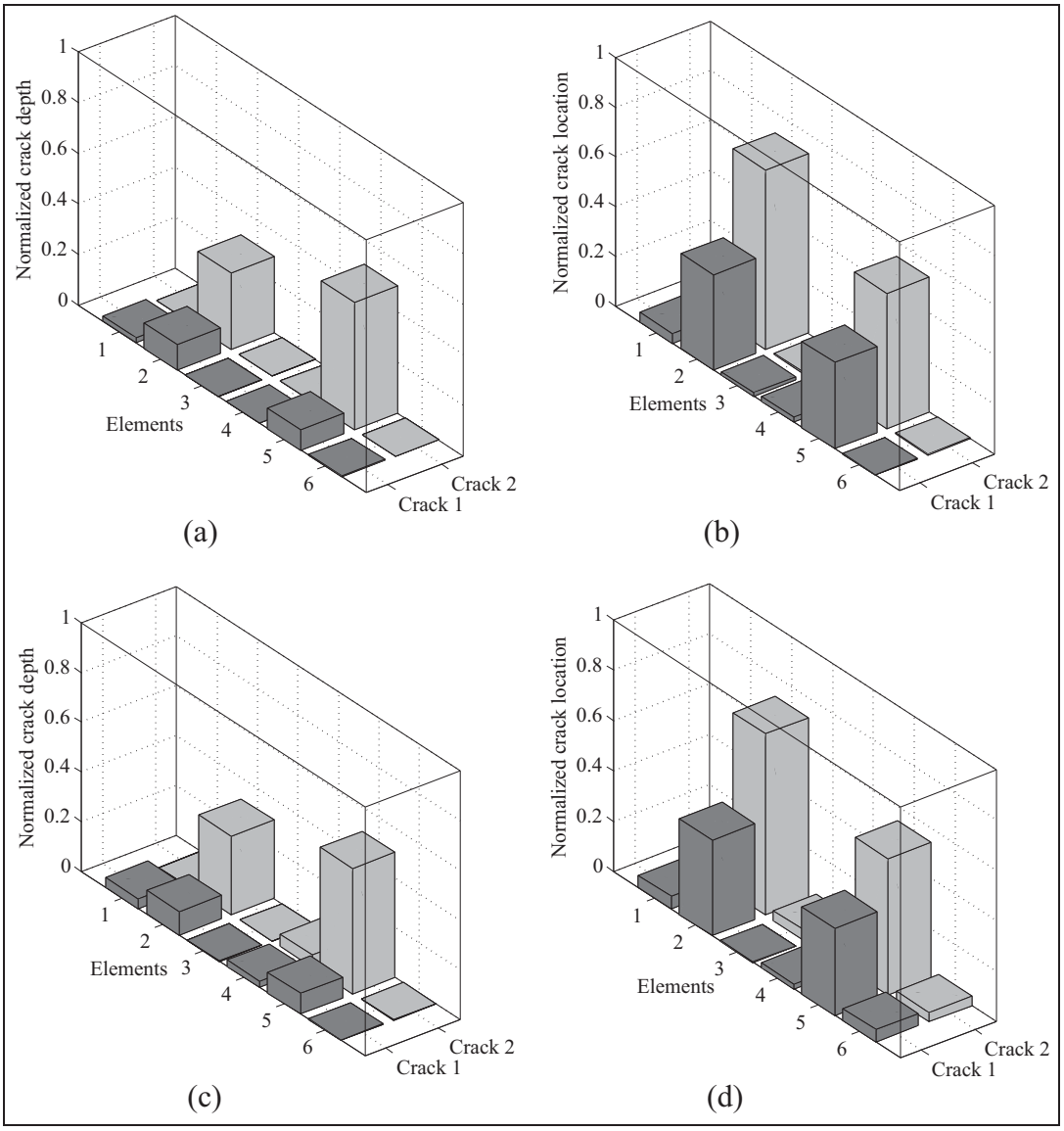

Figure 5. Identified crack parameters of cantilever with complete measurements: (a) identified crack depth (noise free), (b) identified crack location (noise free), (c) identified crack depth (5% noise) and (d) identified crack location (5% noise).

measurement. The method proposed by Viola et al. is capable of detecting only one crack, whereas TM method can able to detect multiple cracks in the structure. The same problem was also solved by Varghese and Shankar[20] using combined acceleration and power flow matching method. They have reported that the percentages of errors in identified crack depth and location were 0.92% and 0.5%, respectively, without noise, and 1.72% and 2.8%, respectively, with 5% noise. The TCTM method identified a crack of depth of 0.5% of beam height with an error of 0.87% in depth and 0.38% in absolute crack location with 5% noisy measurement. The mean computational time taken by the method proposed in Varghese and Shankar[20] is about 3000 s, whereas the mean time taken by the TCTM method is 14 s. This shows that the TCTM method identified multiple cracks in the cantilever and performs better than the other two damage detection methods in terms of accuracy and speed.

Example 2: SS of frame

A frame structure with nine slender beam members is supported as shown in Figure 9(a) used in Nandakumar and Shankar[18] for structural parameter identification (without crack). The cross-section of each member is 12 $\times$ 6 mm. The density of the frame material is 7800 kg/m^3, and its Young's modulus (E) is 200 GPa. The flexural rigidity of the each member is 43.2 N m^2. The first natural frequency of the structure

Downloaded from shm.sagepub.com at UNIVERSITE LAVAL on July 13, 2014

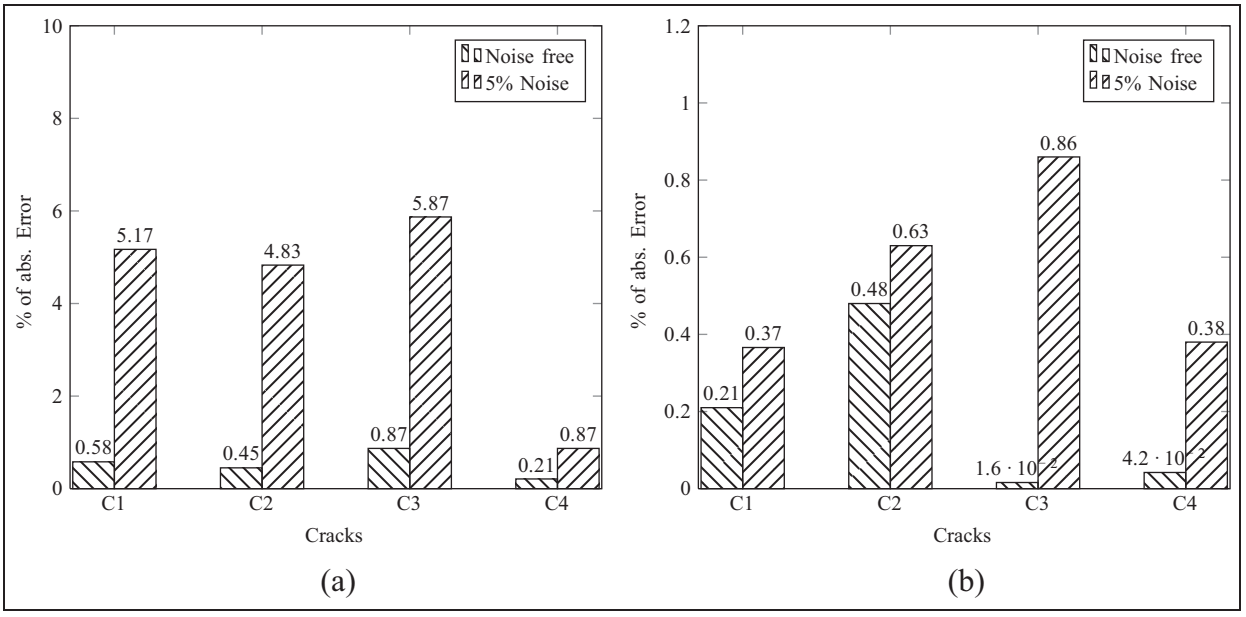

Figure 6. Absolute error in identified parameters of cantilever with complete measurements: (a) depth and (b) location.

is 11.87 Hz. Four open-edge cracks of depth of 0.3, 1.5, 3 and 2 mm are considered at a distance of 362.5, 387.5, 600 and 650 mm, respectively, from the left end of member 4, as shown in Figure 9(b). The normalized crack depths for the above cracks are $\xi_{c1} = 0.05$, $\xi_{c2} = 0.5$, $\xi_{c3} = 0.25$ and $\xi_{c4} = 0.33$, and their normalized locations from the left end of member 4 are $\lambda_{c1} = 0.3625$, $\lambda_{c2} = 0.3875$, $\lambda_{c3} = 0.6$ and $\lambda_{c4} = 0.65$. It is proposed to detect the cracks locally in the SS (member 4) of frame, which is shown inside the dotted box in Figure 9(a). The SS considered is the middle portion of member 4, which has a length of 875 mm and is divided into seven FEs. First two cracks lie on element 3 and the remaining two cracks lie on element 5. The normalized locations of them from the left end of the respective elements are $\lambda_{e3.1} = 0.3$, $\lambda_{e3.2} = 0.4$, $\lambda_{e5.1} = 0.6$ and $\lambda_{e5.2} = 0.7$ ($\lambda_{e3.1}$ means that crack 1 is in element 3). The damping effect in the structure is assumed as Rayleigh's damping model with damping ratio of 1%. The structure is excited by a harmonic force of $10\,sin(2\pi \times 10t)$ N at the midpoint of member 6, which is outside of the SS considered. Hence, the measurement of input force is not required for identification.

In a general structure of this type, the bending moment and shear force in the initial state vector have to be obtained by strain measurements using the relations and procedure discussed in Nandakumar and Shankar[16–18] and is briefly presented here (Figure 10).

$$M(t) = \frac{2EI\varepsilon_B(t)}{h} \tag{22}$$

$$V(t) = \frac{4EI\varepsilon_S(t)}{h^2(1+\nu)} \tag{23}$$

where $M(t)$ and $V(t)$ are bending moment and shear force, respectively, $\varepsilon_B(t)$ and $\varepsilon_S(t)$ are strain due to bending and shear, respectively. The initial state vector $\{X_8\} = \{w_8(t), \theta_8(t), M_8(t), V_8(t)\}^T$ is formed at node 8 of the SS. Translational acceleration is measured at all nodes while angular acceleration, bending moment and shear force responses are measured only at starting node 8. Dynamic strain due to bending $\varepsilon_B(t)$ at the starting node is calculated by measuring the strain at the top and bottom of node 8 as follows

$$\varepsilon_B(t) = \frac{\varepsilon_{top}(t) - \varepsilon_{bot}(t)}{2} \tag{24}$$

where $\varepsilon_{top}(t)$ and $\varepsilon_{bot}(t)$ are the measured dynamic strain at the top- and bottom-bending strain gauges. The crack parameters are identified with responses measured only at nodes 1, 3, 5 and 8. The crack parameters are searched by PSO with swarm size of 50 and 200 iterations per cycle as explained in the incomplete measurement case of the previous example. The identified parameters using incomplete measurements are shown in Figure 11, and the absolute error in those parameters are shown in Figure 12. The crack with smallest depth ($\xi = 0.05$) is identified with an absolute error of 8.75% without noise and 15% with 5% noise in measurement. The location of this crack is identified with an absolute error of 0.2% and 0.27% without and with 5% noise in measurement, respectively. The total time taken for the convergence is 38 s.

Downloaded from shm.sagepub.com at UNIVERSITE LAVAL on July 13, 2014

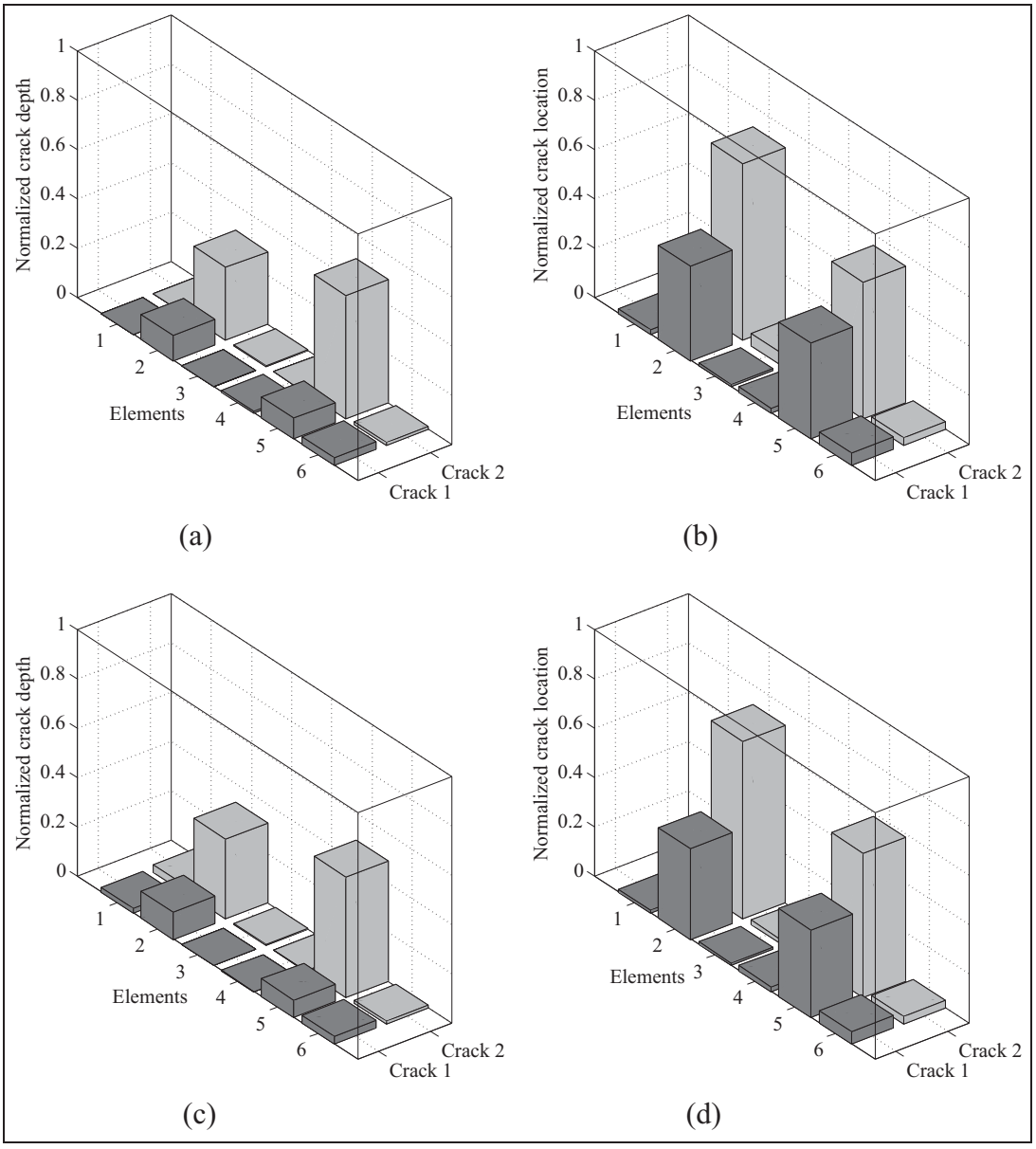

Figure 7. Identified crack parameters of cantilever with incomplete measurements: (a) identified crack depth (noise free), (b) identified crack location (noise free), (c) identified crack depth (5% noise) and (d) identified crack location (5% noise).

Also in this example, the crack with less depth is identified with more error. However, the percentage of error is within the acceptable limit. From this example, it is clear that the TCTM is capable of identifying cracks in any SS with good accuracy and speed. Hence, it is suitable for identifying local crack parameters of any SS without modelling its global structure.

Experimental validation: SS of fixed beam

The TCTM method is experimentally validated by a SS of a fixed beam. A beam made of acrylic material with cross-sectional dimension of 25 × 12 mm and length of 671 mm was fixed at both ends, as shown in Figure 13(a) (same experiment was carried out in Nandakumar and Shankar[17,18] for intact beam). The modulus of elasticity (E) was estimated to be 3.7 GPa from a simple bending test, and the density was measured to be 1190 kg/m^3. The area moment of inertia is calculated from the cross-section of the beam, which is $I = 3.6 \times 10^{-9}$ m^4. The flexural rigidity (EI) of the beam is calculated as 13.32 N m^2. Poisson's ratio (ν) of the beam material is 0.37. Four cracks of depth of 6, 2, 1.5 and 3 mm were introduced on the beam at a

Downloaded from shm.sagepub.com at UNIVERSITE LAVAL on July 13, 2014

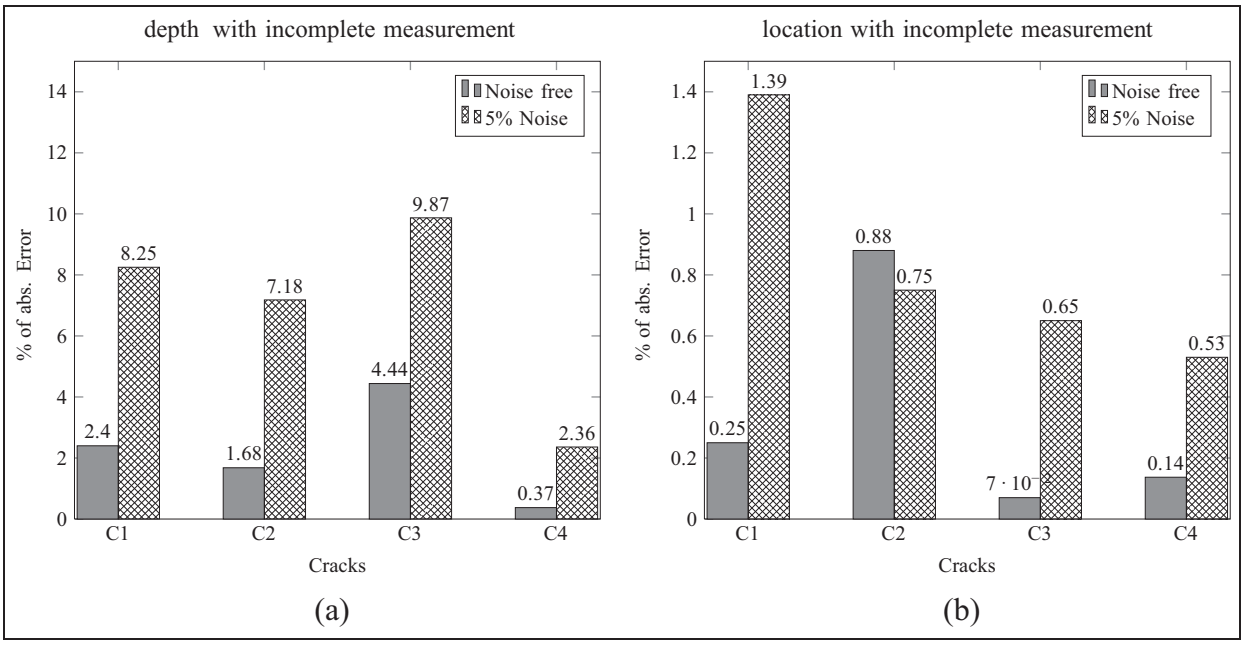

Figure 8. Absolute error in identified parameters of cantilever with incomplete measurements: (a) depth and (b) location.

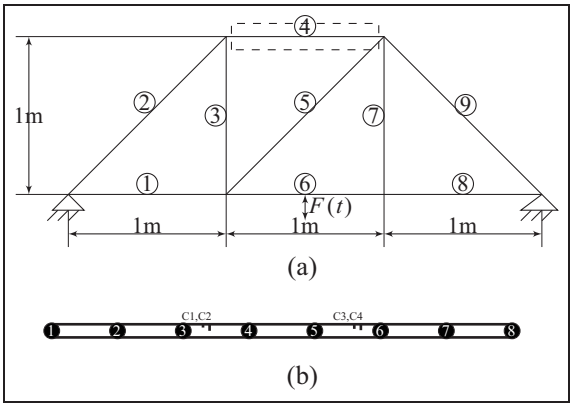

Figure 9. Frame structure: (a) global structure and (b) substructure of member 4 with 8 nodes.

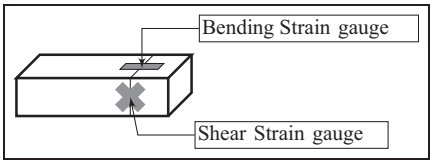

Figure 10. Strain gauge arrangements at starting node.

distance of 265, 278.3, 331.7 and 358.3 mm, respectively, from the left end of the beam. The width of the cracks is about 0.8 mm. The normalized crack depths for the above cracks are $\xi_{c1} = 0.5$, $\xi_{c2} = 0.1667$, $\xi_{c3} = 0.125$ and $\xi_{c4} = 0.25$, respectively. The corresponding normalized crack locations from the left-end support are $\lambda_{c1} = 0.395$, $\lambda_{c2} = 0.4148$, $\lambda_{c3} = 0.4943$ and $\lambda_{c4} = 0.534$, respectively. The natural frequencies for the first two modes of the structure were calculated using the above values of mass and stiffness as 48.1 and 133.28 Hz, respectively. A SS of the beam portion of length 400 mm at a distance of 145 mm from the left end of the beam is considered for damage identification, which is shown in Figure 13(b).

The SS is divided into five FEs each of length 80 mm. The first two cracks $C1$ and $C2$ lie on element 2 and other two cracks $C3$ and $C4$ lie on element 3. The elementwise normalized crack locations are $\lambda_{e2.1} = 0.5$, $\lambda_{e2.2} = 0.667$, $\lambda_{e3.1} = 0.33$ and $\lambda_{e3.2} = 0.667$ measured from the left-end node of the respective element ($\lambda_{e2.1}$ means crack 1 in element 2).

The experimental set-up of fixed beam is shown in Figure 14(a) and the close-up view of the multiple cracks in the beam is shown in Figure 14(b). To measure dynamic response, one DYTRAN miniature accelerometer of 2 gm mass with sensitivity of 107 mV/g and acceleration range of 50 g was fixed at each node to measure translational acceleration, and two accelerometers were fixed at the initial node 1 with centre-to-centre distance of $dx = 7$ mm. The strain gauges and accelerometers arrangement at the starting node to estimate the initial state vector can be seen in Figure 14(c). The shear strain gauges are connected by a half Wheatstone bridge and the two bending strain gauges formed two different quarter Wheatstone bridges. The

Downloaded from shm.sagepub.com at UNIVERSITE LAVAL on July 13, 2014

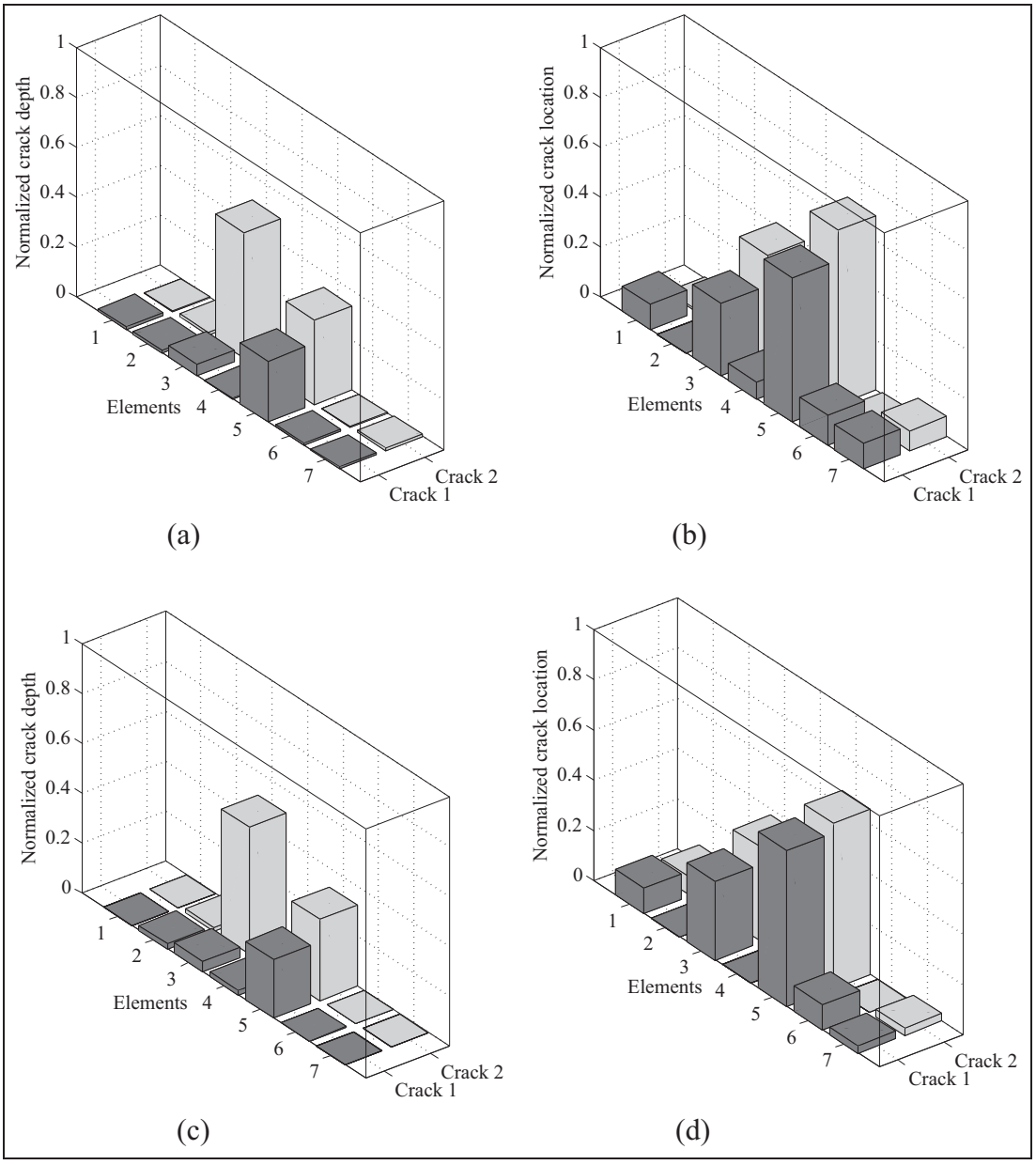

Figure 11. Identified crack parameters of SS of frame structure: (a) identified crack depth (noise free), (b) identified crack location (noise free), (c) identified crack depth (5% noise) and (d) identified crack location (5% noise).
SS: sub-structure.

structure is excited by a sinusoidal force of $2.4\,sin(2\pi 80t)$ N at node 6 by a LDS modal shaker. In this experiment, the initial state vector is measured at a location away from the applied force; this eliminates the requirement of force sensor. A 16-channel DEWE 1201 data acquisition card (DAQ) was used for acquiring data with a sampling frequency of 1000 Hz.

From the acquired data, a portion of data length of 3 s is considered for parameter identification. The angular acceleration at the initial node 1 $(\ddot{\theta}_1(t))$ was calculated by the central difference formula

$$\ddot{\theta}_1(t) = \frac{\ddot{w}_2(t) - \ddot{w}_1(t)}{dx} \tag{25}$$

The translational acceleration at the initial node is the mean value of acceleration measured by two accelerometers. Both translational and angular accelerations were converted into respective displacement responses. The bending moment and shear force responses at the initial node 1 were calculated from the measured bending and shear strain responses using equations (22) and (23) and the state vector at the node 1,

Downloaded from shm.sagepub.com at UNIVERSITE LAVAL on July 13, 2014

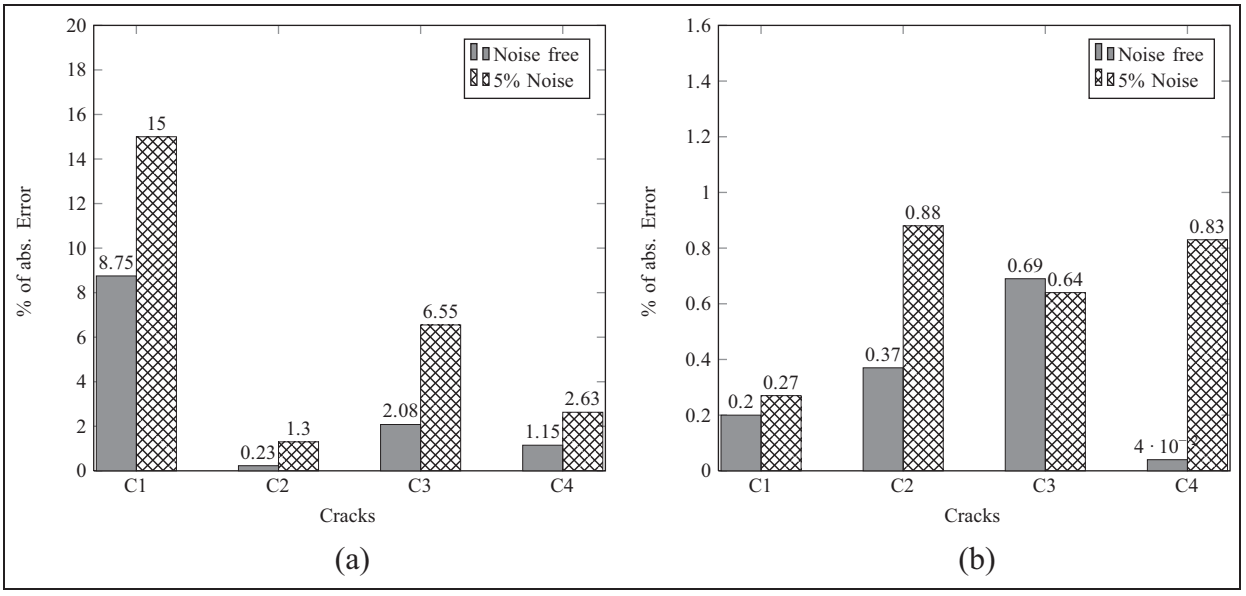

Figure 12. Absolute error in identified parameters in SS of frame: (a) depth and (b) location.
SS: sub-structure.

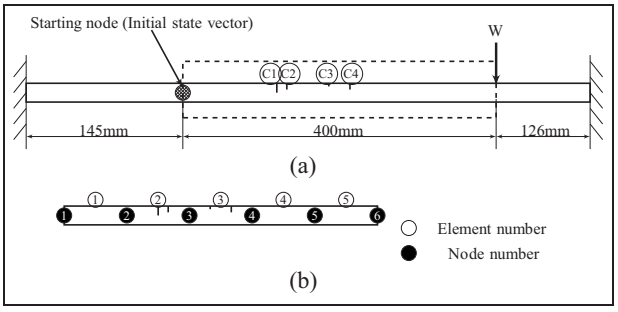

Figure 13. Experimental model of fixed beam: (a) global structure and (b) sub-structure.

$\{X_1\} = \{w_1(t), \theta_1(t), M_1(t), V_1(t)\}^T$ was formed. The crack parameters were searched by PSO with 50 swarm size and 100 iterations for each identification cycle as explained in the previous numerical examples. Cracks were identified from five different sets of readings, and the mean values of identified parameters are shown in Figure 15. The percentage of errors in identified crack depth in the order of cracks shown in Figure 13 are 1.53%, 5.45%, 4.55% and 1.15%, respectively, and the corresponding errors in identified global location are 0.28%, 0.19%, 0.067% and 0.01%, respectively, which are shown in Figure 16. The total CPU time required for convergence is 14 s.

It must be noted that the crack formulation used here (as well as Viola et al.[19]) is applicable for thin cracks, and in the numerical simulation examples, good results were obtained. Hence, the TCTM method proposed here would be able to detect thin cracks. Also, in this experiment, the crack depth of small magnitude has more error in identified values. The strategy of applying TCTM method anywhere in a structure by measuring the initial state vector using strain gauges is proved here. This illustrates the suitability of TCTM method for local identification in a large structure.

Conclusion

A new TM method is proposed in this article to detect multiple cracks in beam-like structures. The TCTM is developed from the FE theory of beam element with two cracks. In simple structures like cantilever, the initial state vector is readily formed at a starting node by measuring displacements, bending moment and shear force responses. However, in a general structure, such as the nine-member frame studied here, the initial state vector has to be obtained by acceleration and strain measurements. Two cracks are assumed in each element, and the successive identification strategy of TCTM method is adopted here since it is fast and accurate. Two numerical examples were studied with complete and incomplete set of measurements. They are a cantilever with multiple cracks and a nine-member structure with multiple cracks (two cracks in each element). The typical error in identified crack parameters ranges from 0.05% (without noise) to 15% (with 5% noise). The TCTM method is validated experimentally by identifying crack parameters of varying depth and location in a SS of a fixed beam with good accuracy. Furthermore, this algorithm is suitable for local

Downloaded from shm.sagepub.com at UNIVERSITE LAVAL on July 13, 2014

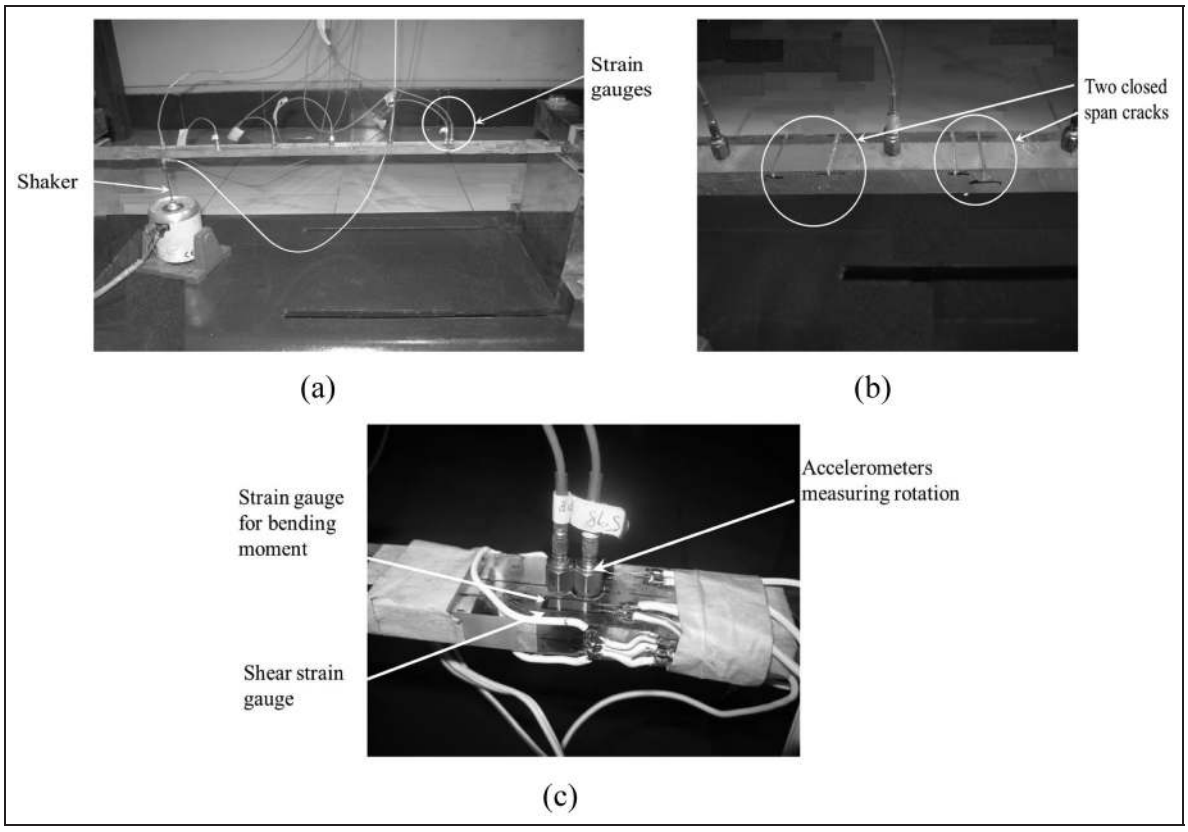

Figure 14. Experimental set-up of fixed beam: (a) global structure, (b) cracks in the beam and (c) strain gauge and accelerometer arrangement at initial node.

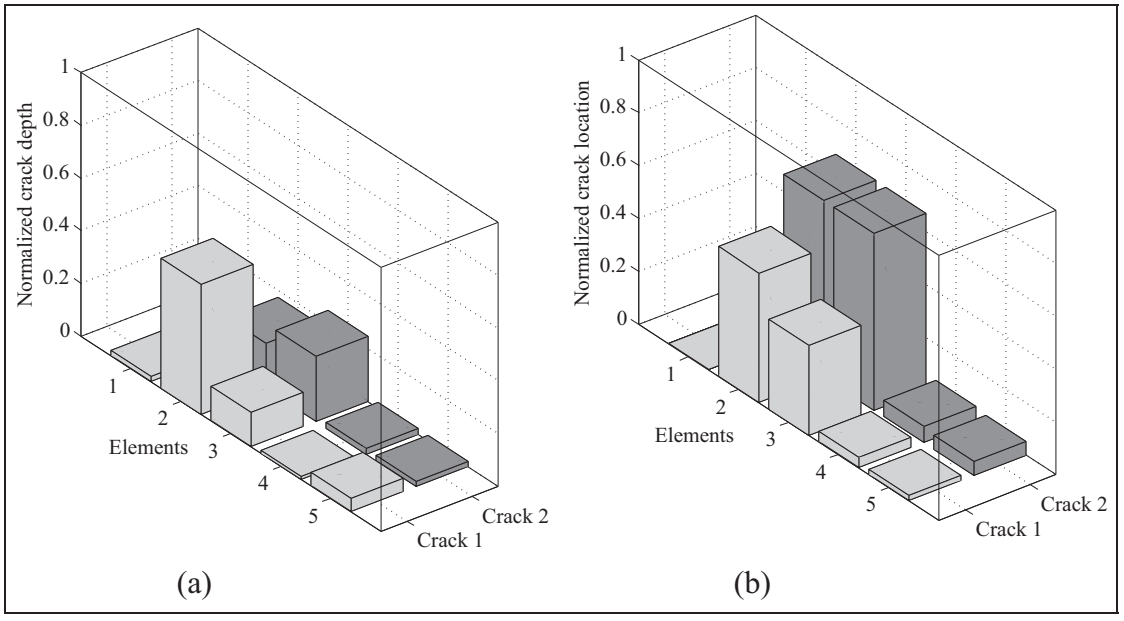

Figure 15. Experimentally identified crack parameters of SS of fixed beam: (a) identified crack depth and (b) identified crack location.
SS: sub-structure.

Downloaded from shm.sagepub.com at UNIVERSITE LAVAL on July 13, 2014

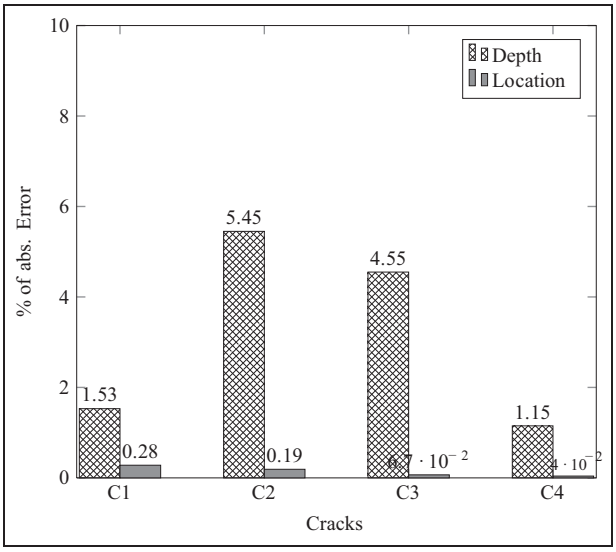

Figure 16. Error in identified parameters of SS of fixed beam.
SS: sub-structure.

damage detection in a large structure, where the initial state vector can be estimated.

Declaration of conflicting interests

The authors declare that there is no conflict of interest.

Funding

This research received no specific grant from any funding agency in the public, commercial or not-for-profit sectors.

References

1. Gounaris G and Dimarogonas A. A finite element of a cracked prismatic beam for structural analysis. *Comput Struct* 1988; 28(3): 309–313.
2. Chondros TG, Dimarogonas AD and Yao J. A continuous cracked beam vibration theory. *J Sound Vib* 1998; 215(1): 17–34.
3. Zheng DY and Kessissoglou NJ. Free vibration analysis of a cracked beam by finite element method. *J Sound Vib* 2004; 273(3): 457–475.
4. Krawczuk M, Zak A and Ostachowicz W. Elastic beam finite element with a transverse elasto-plastic crack. *Finite Elem Anal Des* 2000; 34(1): 61–73.
5. Viola E, Nobile L and Federici L. Formulation of cracked beam element for structural analysis. *J Eng Mech: ASCE* 2002; 128(2): 220–230.
6. Khiem NT and Lien TV. A simplified method for natural frequency analysis of a multiple cracked beam. *J Sound Vib* 2001; 245(4): 737–751.
7. Gounaris GD, Papadopoulos CA and Dimarogonas AD. Crack identification in beams by coupled response measurements. *Comput Struct* 1996; 58(2): 299–305.
8. Krawczuk M. Application of spectral beam finite element with a crack and iterative search technique for damage detection. *Finite Elem Anal Des* 2002; 38(6): 537–548.
9. Gao F and Lu Y. An acceleration residual generation approach for structural damage identification. *J Sound Vib* 2009; 319(1–2): 163–181.
10. Tee KF, Koh CG and Quek ST. Numerical and experimental studies of a substructural identification strategy. *Struct Health Monit* 2009; 8(5): 397–410.
11. Prashanth P and Shankar K. A hybrid neural network strategy for identification of structural parameters. *Struct Infrastruct E* 2010; 6(3): 379–391.
12. Varghese CK and Shankar K. Damage identification using combined transient power flow balance and acceleration matching technique. *Struct Contr Health Monit* 2014; 21: 135–155.
13. Philips AA, Zhishen W and Serker NK. Assessment of vibration-based damage identification methods using displacement and distributed strain measurements. *Struct Health Monit* 2009; 8(6): 443–461.
14. Liew A, Feng NS and Hahn EJ. On using the transfer matrix formulation for transient analysis of nonlinear rotor bearing systems. *Int J Rotat Mach* 2004; 10(6): 425–431.
15. Ghasemalizadeh O, Mirzaee MR, Sadeghi H, et al. Rotor bearing system analysis using the transfer matrix method with thickness assumption of disk and bearing. *Int J Mech Ind Aero Eng* 2008; 2(4): 206–213.
16. Nandakumar P and Shankar K. Estimation of structural parameters using transfer matrices and state vectors. *Int J Appl Sci Eng* 2012; 10(3): 181–207.
17. Nandakumar P and Shankar K. Identification of structural parameters using consistent mass transfer matrix. *Inverse Probl Sci En* 2014; 22: 436–457.
18. Nandakumar P and Shankar K. Structural parameter identification using damped transfer matrix and state vector. *Int J Struct Stab Dy* 2013; 13(4): 1250076 (27 pp.).
19. Viola E, Federici L and Nobile L. Detection of crack location using cracked beam element method for structural analysis. *Theor Appl Fract Mec* 2001; 36(1): 23–35.
20. Varghese CK and Shankar K. Crack identification using combined power flow and acceleration matching technique. *Inverse Probl Sci En* 2012; 20(8): 1239–1257.

Downloaded from shm.sagepub.com at UNIVERSITE LAVAL on July 13, 2014